# Articles

## Synthesis, Structure, and Properties of Molybdenum and Tungsten Cyano Complexes with Cuboidal $M_4(\mu_3\text{-}E)_4$ (M = Mo, W; E = S, Se, Te) Cores

**V. P. Fedin,* I. V. Kalinina, D. G. Samsonenko, Y. V. Mironov, M. N. Sokolov, S. V. Tkachev, A. V. Virovets, and N. V. Podberezskaya**

Institute of Inorganic Chemistry, Russian Academy of Sciences, pr. Lavrentjeva 3, Novosibirsk 630090, Russia

**M. R. J. Elsegood, W. Clegg, and A. G. Sykes***

Department of Chemistry, The University of Newcastle, Newcastle upon Tyne, NE1 7RU, U.K.

*Received August 11, 1998*

Four new tungsten and molybdenum cyano complexes of formula $KCs_5[W_4S_4(CN)_{12}]\cdot CH_3OH\cdot 2H_2O$ (**1**), $K_6[W_4Se_4(CN)_{12}]\cdot 6H_2O$ (**2**), $K_6[W_4Te_4(CN)_{12}]\cdot 5H_2O$ (**3**), and $K_7[Mo_4Te_4(CN)_{12}]\cdot 12H_2O$ (**5**) have been prepared by high-temperature 430−450 °C reaction of the polymeric chain compounds $\{W_3S_7Br_4\}_x$, $\{W_3Se_7Br_4\}_x$, $\{Mo_3Te_7I_4\}_x$ and solid-state $WTe_2$ with KCN, and crystallization from aqueous solutions. In addition $Cs_6[Mo_4Te_4(CN)_{12}]\cdot 2H_2O$ (**4**) has been prepared by oxidation of **5** with bromine water. The molecular structures have been investigated by X-ray crystallography. Mixed-valence (3.5) compounds **1**−**4** are diamagnetic. Mixed-valence (3.25) compound **5** is paramagnetic ($\mu = 2.03\ \mu_B$ at 77 K). In addition to the structural data for these complexes IR and UV−vis spectroscopy have been used to characterize the complexes. Cyclic-voltammetry data have shown that $M_4E_4^{n+}$ (M = Mo, W; E = S, Se, Te) cubes are capable of existing in three oxidation states ranging from the most oxidized ($n = 6$; 10 electrons) to the most reduced electron-precise ($n = 4$; 12 electrons). The $^{77}Se$, $^{125}Te$, and $^{183}W$ NMR spectra of the cubes (**1**−**3**) demonstrate unambiguously the unaltered environments of the W and E atoms in aqueous solution.

### Introduction

The chemistry of metal chalcogen clusters has become a major inorganic growth area.[1−10] Homo- and heterometallic cuboidal clusters with bridging chalcogenide ligands are known for a wide variety of transition metals, and such structures provide an important contribution to studies on transition-metal clusters. Molybdenum and tungsten chalcogenide complexes are relevant in a number of interdisciplinary areas. These range from the bioinorganic chemistry of Mo/S and W/S(Se) containing enzymes[11,12] to the synthesis of highly dispersed/amorphous metal chalcogenides, which are important catalysts for hydrogenation/dehydrogenation reactions as well as C−S bond hydrogenation, i.e. crude-oil hydrodesulfurization (HDS) processes.[13,14] Recently polymeric chain compounds $\{M_3E_7Br_4\}_x$, containing M = Mo, W and chalcogenide/polychalcogenide ligands (E), have been prepared by self-assembly processes involving heating stoichiometric mixtures of the elements. An increasingly important property of these starting compounds which have chain-linked units is their potential to give single molecular $M_3$ or $M_4$ clusters.

Homometallic $Mo_4S_4$ cuboidal clusters of general formula $[Mo_4S_4L_{12}]$, with ligands L either neutral or anionic, have been known for some 20 years.[1,3−6,8,9,15,16] The oxidation states of molybdenum vary from III to V. Cuboidal-type molecular clusters with $Mo_4Se_4^{n+}$ cores ($n = 4, 5, 6$) have also been reported.[17,18] As compared with molybdenum the number of $W_4$ chalcogenide complexes is limited; examples are (a) the raft-

(1) Holm, R. H. *Adv. Inorg. Chem.* **1992**, *38*, 1.
(2) Coucouvanis, D. *Acc. Chem. Res.* **1991**, *24*, 1.
(3) Saito, T. In *Early Transition Metal Clusters with π-Donor Ligands*; Chisholm, M. H., Ed.; VCH Publishers: New York, 1995; p 63.
(4) Dance, I.; Fisher, K. *Prog. Inorg. Chem.* **1994**, *41*, 637.
(5) Shibahara, T. *Adv. Inorg. Chem.* **1991**, *30*, 143.
(6) Shibahara, T. *Coord. Chem. Rev.* **1993**, *123*, 73.
(7) Roof, L. C.; Kolis, J. W. *Chem. Rev.* **1993**, *93*, 1037.
(8) Müller, A. *Polyhedron* **1986**, *5*, 323.
(9) Müller, A.; Jostes, R.; Cotton, F. A. *Angew. Chem., Int. Ed. Engl.* **1980**, *19*, 875.
(10) Fedorov, V. E.; Mischchenko, A. V.; Fedin, V. P. *Russ. Chem. Rev.* **1985**, *54*, 408.
(11) Spiro, T. G. *Molybdenum Enzymes*; Wiley: New York, 1985. Rees, D. C.; Chan, M. K.; Kim, J. *Adv. Inorg. Chem.* **1994**, *40*, 89.
(12) Enemark, J. H.; Young, C. G. *Adv. Inorg. Chem.* **1994**, *40*, 2.
(13) Topsoe, H.; Massoth, F. E.; Clausen, B. S. In *Catalysis, Science and Technology*; Anderson, J. R., Boudart, M., Eds.; Springer-Verlag, 1996; Vol. 11.
(14) Topsoe, H.; Clausen, B. S. *Catal. Rev.—Sci. Eng.* **1984**, *26*, 395.
(15) Harris, S. *Polyhedron* **1989**, *8*, 2843.
(16) Saito, T. *Adv. Inorg. Chem.* **1996**, *44*, 45.
(17) Nasreldin, M.; Henkel, G.; Kampmann, G.; Krebs, B.; Lamprecht, G. J.; Routledge, C. A.; Sykes, A. G. *J. Chem. Soc., Dalton Trans.* **1993**, 737.
(18) McFarlane, W.; Nasreldin, M.; Saysell, D. M.; Jia, Z.-S.; Clegg, W.; Elsegood, M. R. J.; Murray, K. S.; Moubaraki, B.; Sykes, A. G. *J. Chem. Soc., Dalton Trans.* **1996**, 363 and references therein.

10.1021/ic980956z CCC: $18.00 
Published on Web 04/03/1999

type complex $[W_4S_6(SH)_2(PMe_2Ph)_6]$,[19,20] (b) the tetrahedral complex $[W_4S_6(PMe_2Ph)_4]$ with a $W_4(\mu_2\text{-}S)_6$ adamantane-like core,[19,20] (c) $[W_4S_8(H_2NCH_2CH_2NH_2)_4]S$ having a cuboidal $W_4S_4^{10+}$ core,[21] (d) the W(V) complex $\{W(NC_6H_4CH_3)(S_2P(OC_2H_5)_2(\mu_3\text{-}S)\}_4$, which in solution is formed by an associative equilibrium of two dimers,[22] and (e) $\beta$-$[W_4S_4(\mu\text{-dtp})_2(dtp)_4]$ and $\alpha$-$[W_4S_4(\mu\text{-dtp})_3(dtp)_3]$ with cuboidal-type $W_4S_4^{6+}$ cores (dtp = dithiaphosphate).[23]

Solid-state molybdenum compounds $Mo_4S_4X_4$ (X = Cl, Br, I) and $M'Mo_4E_8$ (M′ = Al, Ga, E = S; M′ = Ga, E = Se) are known to contain $[Mo_4E_4]$ cores, with each Mo octahedrally coordinated by three chalcogen and three halogen atoms, or six chalcogen atoms.[24−27] However, solid-state tungsten analogues are hitherto unknown. There are comparatively few tungsten chalcogenide cuboidal clusters, which is curious in view of the number of molybdenum examples. The number of telluride-containing clusters is also relatively small. There is also considerable interest in comparing the properties of molybdenum and tungsten chalcogenide complexes, especially in cases where isostructural complexes are known.

In the course of our studies on the synthesis and reactivities of solid-state molybdenum and tungsten chalcogenides, we have recently obtained the first complexes with cuboidal $M_4Te_4$ (M = Mo, W) cores $K_7[Mo_4(\mu_3\text{-}Te)_4(CN)_{12}]\cdot 12H_2O$ and $K_6[W_4(\mu_3\text{-}Te)_4(CN)_{12}]\cdot 5H_2O$, reported in a short communication.[28] We describe here detailed synthetic procedures, X-ray structure determinations, and properties of the cuboidal $W_4S_4$, $W_4Se_4$, $W_4Te_4$, and $Mo_4Te_4$ clusters as cyano complexes.

## Experimental Section

**Procedural Details.** Isolation and purification of the molybdenum and tungsten cyano complexes (Figure 1) were carried out in air. All reagents were of analytical grade purity. Potassium thiocyanate was first dried at 200 °C in a vacuum. The polymeric chain compounds $\{M_3E_7Br_4\}_x$ (M = Mo, W; E = S, Se),[29−31] $\{Mo_3Te_7I_4\}_x$,[32] and solid-state $WTe_2$[33] were prepared by direct combination of the elements.

Tungsten, molybdenum, and tellurium were determined by atomic absorption spectroscopy on a Perkin-Elmer 303 or Hitachi 2-8000 instrument. Potassium and cesium were determined by an atomic emission method on an Hitachi 2-8000 spectrometer, and C,H,N,S analyses were performed on a Carlo Erba 1106.

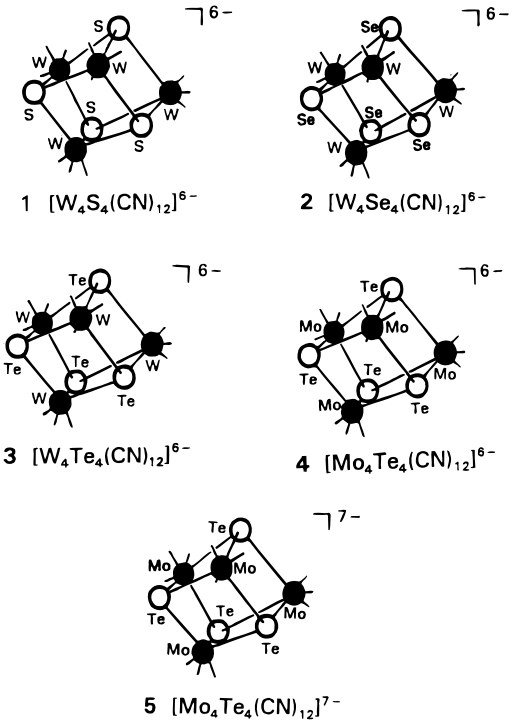


**Figure 1.** Schematic structures of cubes relevant to this paper.

The IR spectra were recorded from KBr disks and from Nujol mulls between KBr plates, using an IFS-85 spectrometer (Bruker). UV−vis spectra (300−1100 nm) were recorded on a Shimadzu UV-1202 spectrophotometer. To measure magnetic susceptibility the Faraday method was used. X-ray powder diffraction diagrams were obtained on a Philips APD 1700 machine. For the determination of water content, thermal gravimetric mass loss procedures were employed, heating rate 5 °C/min, in an Ar atmosphere using a TGD-7000RH thermal analysis controller (Japan, Sinku-Riko).

Cyclic-voltammetry measurements were carried out on a CV-50W workstation. The working and counter electrodes used were glassy carbon disk and Pt wire, respectively. Cyclic voltammograms were recorded at room temperature in aqueous solutions containing 0.10 M $Na_2SO_4$ at a 100 mV/s scan rate. Sample solutions (ca. 1 mM) were deoxygenated with a stream of $N_2$ gas. All reduction potentials were referenced against the normal hydrogen electrode (NHE). An Ag/AgCl reference electrode was calibrated against the $[Fe(CN)_6]^{3-/4-}$ couple in 0.10 M $Na_2SO_4$, reduction potential 360 mV vs NHE.

Solutions of **1** (0.13 M), **2** (0.12 M), and **3** (0.066−0.266 M) in $H_2O$ were used for NMR measurements. The $^{77}$Se, $^{125}$Te, and $^{183}$W NMR spectra were obtained at frequencies of 57.3, 94.7, and 12.2 MHz, respectively, on a Bruker CXP-300 spectrometer using 10 mm outside diameter tubes. For $^{77}$Se spectra the width was 8 kHz, the pulse-repetition interval was 11.0 $\mu$s, and chemical shifts were referenced against an external standard of saturated aqueous $H_2SeO_3$ solution at $\delta$ = 1282 ppm.[34] A total shift range from 1000 to 1500 ppm was examined for $^{77}$Se NMR spectra. For $^{125}$Te spectra the spectral width was 25 kHz, the pulse-repetition interval was 19.0 $\mu$s, and chemical shifts were referenced to the external standard saturated aqueous solution of $H_6TeO_6$ at $\delta$ = 712 ppm.[34] A total shift range from −1000 to 2200 ppm was examined for $^{125}$Te NMR spectra. For $^{183}$W spectra the spectral width was 5−10 kHz, the pulse-repetition interval was 22.0 $\mu$s, and chemical shifts were measured relative to the external standard $H_4SiW_{12}O_{40}$ at $\delta$ = −103.5 ppm.[35] A total shift range from −2000 to 3000 ppm was examined for $^{183}$W NMR spectra.

**Preparation of $KCs_5[W_4(\mu_3\text{-}S)_4(CN)_{12}]\cdot CH_3OH\cdot 2H_2O$ (1).** A mixture of $\{W_3S_7Br_4\}_x$ (2.00 g; 1.82 mmol) and KCN (2.00 g; 30.7

(19) Kuwata, S.; Mizobe, Y.; Hidai, M. *J. Chem. Soc., Chem. Commun*. **1995**, 1057.
(20) Kuwata, S.; Mizobe, Y.; Hidai, M. *J. Chem. Soc., Dalton Trans*. **1997**, 1753.
(21) Wood, P. T.; Pennington, W. T.; Kolis, J. W.; Wu, B.; O'Connor, C. J. *Inorg. Chem.* **1993**, *32*, 129.
(22) Sampson, M. L.; Richardson, J. F.; Noble, M. E. *Inorg. Chem*. **1992**, *31*, 2726.
(23) Lu, S.-F.; Huang, J.-Q.; Zhuang, H.-H.; Li, J.-Q.; Wu, D.-M.; Huang, Z.-X.; Lu, C.-Z.; Huang, J.-L.; Lu, J.-X. *Polyhedron* **1991**, *10*, 2203.
(24) Perrin, C.; Chevrel, R.; Sergent, M. *C. R. Seances Acad. Sci.* **1975**, *280*, 949.
(25) Vandenberg, J. M.; Brasen, D. J. *Solid State Chem*. **1975**, *14*, 203.
(26) Perrin, C.; Chevrel, R.; Sergent, M. *C. R. Seances Acad. Sci.* **1975**, *281*, 23.
(27) LeBeuze, A.; Zerrovski, M. C.; Loirat, H.; Lissillour, R. *J. Alloys Compd*. **1992**, *190*, 1.
(28) Fedin, V. P.; Kalinina, I. V.; Virovets, A. V.; Podberezskaya, N. V.; Sykes, A. G. *Chem. Commun*. **1998**, 237.
(29) Fedin, V. P.; Sokolov, M. N.; Virovets, A. V.; Podberezskaya, N. V.; Fedorov, V. Ye. *Polyhedron* **1992**, *11*, 2973.
(30) Fedin, V. P.; Sokolov, M. N.; Gerasko, O. A.; Kolesov, B. A.; Fedorov, V. Ye.; Mironov, A. V.; Yufit, D. S.; Slovohotov, Yu. L.; Struchkov, Yu. T. *Inorg. Chim. Acta* **1990**, *175*, 217.
(31) Fedin, V. P.; Sokolov, M. N.; Myakishev, K. G.; Gerasko, O. A.; Fedorov, V. Ye.; Macicek, J. *Polyhedron* **1991**, *10*, 1311.
(32) Fedin, V. P.; Imoto, H.; Saito, T.; McFarlane, W.; Sykes, A. G. *Inorg. Chem*. **1995**, *34*, 5097.
(33) Brixner, L. H. *J. Inorg. Nucl. Chem*. **1962**, *24*, 257.
(34) Mann, B. E., Harris, R. K., Eds. *NMR and the Periodic Table*; Acad. Press: London, 1978.
(35) Fedotov, M. A. *Nuclear Magnetic Resonance in Solutions of Inorganic Compounds* (in Russian); Nauka: Novosibirsk, USSR, 1987.

mmol) was heated (430 °C; 48 h) in a sealed Pyrex tube. The product of the reaction was added to 40 mL of water and the mixture refluxed for 1 h. After filtration, the solution was kept in an open beaker (100 mL) at atmospheric pressure and ~80 °C. During this time (2−4 h), the volume decreased to 10 mL. After addition of methanol (40 mL) at 20 °C a brown precipitate formed and was filtered off and washed with 80% methanol. The product was dissolved in 20 mL of water, and 0.50 g of CsCl was added to the solution. Dark red-brown crystals of **1** were obtained by slow diffusion (3−7 days) of methanol into the aqueous solution. The crystals were filtered off, washed with methanol, and dried in air. Yield: 0.78 g of **1** (22%). The yield is less if heating is to 450 °C. Anal. Calcd for $C_{13}H_8N_{12}O_3Cs_5KS_4W_4$: C, 8.02; H, 0.41; N, 8.63; S, 6.58. Found: C, 7.65; H, 0.45; N, 8.77; S, 6.64. IR (as KBr pellet): 3600(s), 2125(s), 1613(m), 1086(w), 892(w), 410(m) $cm^{-1}$. The UV−vis absorption spectrum of **1** in $H_2O$ gave peak positions $\lambda$/nm ($\epsilon$/$M^{-1}$ $cm^{-1}$) at 362sh, 460sh (1530), 789 (400). To ensure product homogeneity, the X-ray powder diffraction diagram of **1** was obtained and found to be identical with that calculated from the single-crystal data (see below).

The magnetic susceptibility of **1** was measured at 300 K: $\chi_M = -377 \times 10^{-5}$ $cm^3$ $mol^{-1}$.

**Preparation of $K_6[W_4(\mu_3\text{-}Se)_4(CN)_{12}]\cdot 6H_2O$ (2).** A mixture of $\{W_3Se_7Br_4\}_x$ (3.00 g; 2.11 mmol) and KCN (3.00 g; 46.0 mmol) was heated (450 °C; 48 h) in a sealed Pyrex tube. The product of the reaction was added to 40 mL of water and the mixture refluxed for 2 h. After filtration, the solution was kept at 80 °C. During this time, the volume was decreased to 7 mL. After the mixture was allowed to stand at 20 °C for 3−7 days, dark red-brown crystals were separated by filtration, washed with 80% methanol, and dried in air. Yield: 0.50 g of $K_6[W_4(\mu_3\text{-}Se)_4(CN)_{12}]\cdot 6H_2O$ (14%). Anal. Calcd for $C_{12}H_{12}N_{12}O_6K_6Se_4W_4$: C, 8.45; H, 0.71; N, 9.85; Se, 18.51. Found: C, 8.35; H, 0.77; N, 9.99; Se, 18.50. IR (KBr): 3570(s), 2116(s), 1616(m), 827(w), 420(m) $cm^{-1}$. The UV−vis absorption spectrum of **2** in $H_2O$ gave peak positions $\lambda$/nm ($\epsilon$/$M^{-1}$ $cm^{-1}$) at 314 (15 400), 385 (4800), 490sh (1250), 850 (370).

The magnetic susceptibility of **2** was measured at 300 K: $\chi_m = -345 \times 10^{-5}$ $cm^3$ $mol^{-1}$.

**Preparation of $K_6[W_4(\mu_3\text{-}Te)_4(CN)_{12}]\cdot 5H_2O$ (3).** A mixture of $WTe_2$ (5.00 g; 11.4 mmol) and KCN (5.0 g; 76.8 mmol) was heated (450 °C; 48 h) in a sealed Pyrex tube. The product of the reaction was added to 70 mL of water, and the mixture was refluxed for 3 h. After filtration, the solution was kept at 80 °C. During this time, the volume was decreased to 7 mL. After the mixture was allowed to stand at 20 °C for 1−3 days, the dark red-brown crystals were isolated by filtration and dried in air. Yield: 4.73 g of $K_6[W_4(\mu_3\text{-}Te)_4(CN)_{12}]\cdot 5H_2O$ (88%). Anal. Calcd for $C_{12}H_{10}N_{12}O_5K_6Te_4W_4$: C, 7.66; H, 0.54; N, 8.93; K, 12.46; Te, 27.11; W, 39.06; $H_2O$, 4.78. Found: C, 7.94; H, 0.51; N, 8.36; K, 11.98; Te, 26.79; W, 39.80; $H_2O$, 4.99. To demonstrate product homogeneity, the X-ray powder diffraction diagram of **3** was obtained and found to be identical with the diagram calculated from the single-crystal data (see below). IR (as KBr pellet): 3560(s), 2097(s), 1616(m) 1000(w), 912(w), 818(w), 756(w), 426(m) $cm^{-1}$. IR (Nujol): 2098(s) $cm^{-1}$. The UV−vis absorption spectrum of **3** in $H_2O$ gave peak positions $\lambda$/nm ($\epsilon$/$M^{-1}$ $cm^{-1}$) at 357 (8000), 382sh, 474 (3140), 869 (440).

The magnetic susceptibility of **3** was measured at 300 K: $\chi_m = -360 \times 10^{-5}$ $cm^3$ $mol^{-1}$.

**Preparation of $Cs_6[Mo_4(\mu_3\text{-}Te)_4(CN)_{12}]\cdot 2H_2O$ (4).** A few drops of bromine water were added to the solution of 0.20 g of $K_7[Mo_4(\mu_3\text{-}Te)_4(CN)_{12}]\cdot 11H_2O$ (**5**) in 20 mL of water. Addition of cesium chloride (0.20 g) and slow diffusion of methanol to the solution (2−3 days) gives rise to the formation of red-brown crystals, which were filtered off, washed with methanol, and dried in air. Yield: 0.23 g of $KCs_5[Mo_4(\mu_3\text{-}Te)_4(CN)_{12}]\cdot 2H_2O$ (92%). Anal. Calcd for $C_{12}H_4N_{12}O_2Cs_5KMo_4Te_4$: Cs, 34.15; K, 2.01; Mo, 19.72; Te, 26.23. Found: Cs, 33.15; K, 2.01; Mo, 19.70; Te, 26.03. Recrystallization of $KCs_5[Mo_4(\mu_3\text{-}Te)_4(CN)_{12}]\cdot 2H_2O$ from 10% CsCl gives pure cesium salt $Cs_6[Mo_4(\mu_3\text{-}Te)_4(CN)_{12}]\cdot 2H_2O$ (**4**). IR (as KBr pellet): 3380(s), 2102(s), 1624(m), 1090(w), 1050(w), 882(w), 403(m) $cm^{-1}$. The UV−vis absorption spectrum of **4** in $H_2O$ gave peak positions $\lambda$/nm ($\epsilon$/$M^{-1}$ $cm^{-1}$) at 388 (4500), 521 (1780), 947 (200).

The magnetic susceptibility of **4** was measured at 300 K: $\chi_m = -334 \times 10^{-5}$ $cm^3$ $mol^{-1}$.

**Preparation of $K_7[Mo_4(\mu_3\text{-}Te)_4(CN)_{12}]\cdot 12H_2O$ (5).** A mixture of $\{Mo_3Te_7I_4\}_x$ (3.00 g; 1.78 mmol) and KCN (3 g; 46 mmol) was heated (450 °C; 48 h) in a sealed quartz tube. The product of the reaction was added to 50 mL of water, and the mixture was refluxed for 3 h. After filtration, the solution was kept at 80 °C. During this time, the volume was decreased to 10 mL. After the mixture was allowed to stand at 20 °C for 1 day, the dark red-brown crystals together with colorless powder were isolated by filtration, washed with cool water (to remove colorless powder), and dried in air. Yield: 1.86 g of $K_7[Mo_4(\mu_3\text{-}Te)_4(CN)_{12}]\cdot 12H_2O$ (83%). Anal. Calcd for $C_{12}H_{24}N_{12}O_{12}Mo_4K_7Te_4$: C, 8.50; H, 1.43; N, 9.91; Mo, 22.62; K, 16.13; Te, 30.09; $H_2O$, 12.75. Found: C, 9.18; H, 1.70; N, 9.88; Mo, 23.46; K, 16.30; Te, 30.21; $H_2O$, 12.17. To demonstrate product homogeneity, the X-ray powder diffraction diagram of **5** was obtained and found to be identical with the diagram calculated from the single-crystal data (see below). IR (as KBr pellet): 3450(s), 2086(s), 1617(m), 1080(w), 425(w) $cm^{-1}$. IR (Nujol): 2084 $cm^{-1}$. The UV−vis absorption spectrum of **5** in $H_2O$ gave peak positions $\lambda$/nm ($\epsilon$/$M^{-1}$ $cm^{-1}$) at 382 (6100), 535 (2080), 769 (420).

The magnetic susceptibility of **5** was measured at 77 K ($\mu = 2.03$ $\mu_B$) and 300 K ($\mu = 2.17$ $\mu_B$).

**Preparation of $K_6[W_4(\mu_3\text{-}S)_4(CN)_{12}]\cdot 4H_2O$ from $WTe_2$ and $SCN^-$.** A mixture of $WTe_2$ (2.00 g; 4.56 mmol) and KSCN (2.00 g; 20.4 mmol) was heated (450 °C; 48 h) in a sealed Pyrex tube. The product of the reaction was added to 40 mL of water, and the mixture was refluxed for 2 h. After filtration, the solution was kept at 80 °C. During this time, the volume was decreased to 7 mL. After addition of methanol (50 mL) at 20 °C, brown precipitate was filtered off, washed with 80% methanol, and dried in air. Yield: 0.38 g of $K_6[W_4(\mu_3\text{-}S)_4(CN)_{12}]\cdot 4H_2O$ (23%). Anal. Calcd for $C_{12}H_8N_{12}O_4K_6S_4W_4$: C, 9.72; H, 0.54; N, 11.34; K, 15.82; S, 8.65; W, 49.60. Found: C, 9.65; H, 0.46; N, 11.30; K, 16.32; S, 8.66; W, 49.57.

**Crystallographic Studies.** Crystal data are given in Table 1, and further details of the structure refinement and calculations are in the Supporting Information.

A crystal of **1** was examined on a Bruker AXS CCD area-detector diffractometer. Intensities were integrated from more than a hemisphere of data recorded on 0.3° frames by $\omega$ rotation; cell parameters were refined from the observed rotation angles of all strong reflections. Semiempirical absorption corrections were applied, based on symmetry-equivalent and repeated data.

Crystals of **2**−**5** were examined on an Enraf-Nonius CAD4 diffractometer. Intensities were measured variously by $\omega$ or $\theta/2\theta$ scans; cell parameters were refined in each case from 24 centered reflections. Absorption corrections were by numerical integration (**2**) or based on azimuthal scans (**3**−**5**).

The structures were solved by direct methods and refined by least-squares methods on all unique $F^2$ values, with anisotropic displacement parameters, and with no inclusion of H atoms. Some cation disorder was resolved for **2** and **5**. The absolute structure of the non-centrosymmetric **4** was determined by refinement of the enantiopole parameter[36] to −0.03(9). The largest features in final difference syntheses were close to heavy atoms and disorder sites. Programs were standard Bruker AXS and Enraf-Nonius control and integration software and members of the SHELX family (Bruker AXS Inc., Madison, WI, and G. M. Sheldrick, University of Göttingen, Germany). Selected bond lengths and angles are listed in Tables 2−6. Complete results can be found in the Supporting Information.

## Results and Discussions

**Synthesis of Cyano Complexes.** Preparative routes used previously to obtain $Mo_4E_4^{n+}$ cuboidal clusters (E = S, Se), $n$ = 4, 5, and 6, include dimerization of chalcogenide $Mo_2$ complexes and addition of a mononuclear complex to a $Mo_3$ triangular chalcogenide complex.[37,38] Self-assembly routes have

(36) Flack, H. D. *Acta Crystallogr., Sect. A* **1983**, *39*, 876.
(37) Martinez, M.; Ooi, B.-L.; Sykes, A. G. *J. Am. Chem. Soc.* **1987**, *109*, 4615.

**Table 1.** Crystallographic Data for **1**−**5**

| | **1** | **2** | **3** | **4** | **5** |
|---|---|---|---|---|---|
| formula | $C_{13}H_8Cs_5KN_{12}O_3S_4W_4$ | $C_{12}H_{12}K_6N_{12}O_6Se_4W_4$ | $C_{13}H_{10}K_6N_{12}O_5Te_4W_4$ | $C_{12}H_4Cs_6Mo_4N_{12}O_2Te_4$ | $C_{12}H_{24}K_7Mo_4N_{12}O_{12}Te_4$ |
| fw | 1947.6 | 1706.2 | 1882.7 | 2039.9 | 1696.3 |
| space group | $P2_1/c$ | $Cmma$ | $P\bar{1}$ | $P2_1$ | $Pnma$ |
| $Z$ | 4 | 4 | 2 | 2 | 4 |
| $a$, Å | 18.116(4) | 14.175(1) | 12.399(1) | 11.617(1) | 12.112(1) |
| $b$, Å | 10.335(3) | 21.298(2) | 13.187(1) | 10.124(2) | 21.736(2) |
| $c$, Å | 19.414(5) | 13.725(2) | 13.496(1) | 17.473(4) | 16.109(1) |
| α, deg | | | 83.712(8) | | |
| $\beta$, deg | 95.568(7) | | 66.575(8) | 100.75(1) | |
| $\gamma$, deg | | | 63.223(9) | | |
| $V$, Å$^3$ | 3618(2) | 4143.6(8) | 1801.1(2) | 2018.9(6) | 4241.0(6) |
| $\rho_{calcd}$, g cm$^{-3}$ | 3.574 | 2.735 | 3.471 | 3.356 | 2.657 |
| $T$, °C | −100 | 20 | 20 | 20 | 20 |
| $\lambda$, Å | 0.710 73 | 0.710 73 | 0.710 73 | 0.710 73 | 0.710 73 |
| $\mu$, cm$^{-1}$ | 180.2 | 152.3 | 166.4 | 94.1 | 46.0 |
| $R(F_o)^a$ | 0.0451 | 0.0473 | 0.0696 | 0.0634 | 0.0471 |
| $R_w(F_o^2)^b$ | 0.0951 | 0.1558 | 0.2213 | 0.1542 | 0.1253 |

[a] $R = \sum||F_o| - |F_c||/\sum|F_o|$ for "observed" reflections having $F_o^2 > 2\sigma(F_o^2)$. [b] $R_w = [\sum w(F_o^2 - F_c^2)^2/\sum w(F_o^2)^2]^{1/2}$ for all data.

**Table 2.** Selected Bond Lengths (Å) and Angles (deg) for **1**

| | | | |
|---|---|---|---|
| W(1)−W(2) | 2.8914(8) | W(1)−W(3) | 2.7994(8) |
| W(1)−W(4) | 2.8212(8) | W(2)−W(3) | 2.8209(9) |
| W(2)−W(4) | 2.8351(8) | W(3)−W(4) | 2.9038(9) |
| W(1)−S(1) | 2.400(3) | W(1)−S(2) | 2.377(3) |
| W(1)−S(3) | 2.407(3) | W(2)−S(1) | 2.400(3) |
| W(2)−S(3) | 2.388(3) | W(2)−S(4) | 2.395(3) |
| W(3)−S(1) | 2.375(3) | W(3)−S(2) | 2.402(3) |
| W(3)−S(4) | 2.403(3) | W(4)−S(2) | 2.386(3) |
| W(4)−S(3) | 2.390(3) | W(4)−S(4) | 2.405(3) |
| W(1)−C(1) | 2.184(12) | W(1)−C(2) | 2.160(12) |
| W(1)−C(3) | 2.165(11) | W(2)−C(4) | 2.203(11) |
| W(2)−C(5) | 2.172(12) | W(2)−C(6) | 2.186(11) |
| W(3)−C(7) | 2.157(12) | W(3)−C(8) | 2.194(11) |
| W(3)−C(9) | 2.175(12) | W(4)−C(10) | 2.177(13) |
| W(4)−C(11) | 2.160(11) | W(4)−C(12) | 2.185(12) |
| C(2)−W(1)−C(3) | 79.5(4) | C(2)−W(1)−C(1) | 80.7(4) |
| C(3)−W(1)−C(1) | 81.2(4) | C(5)−W(2)−C(6) | 78.8(4) |
| C(5)−W(2)−C(4) | 80.2(4) | C(6)−W(2)−C(4) | 79.2(4) |
| C(7)−W(3)−C(9) | 77.7(4) | C(7)−W(3)−C(8) | 80.4(4) |
| C(9)−W(3)−C(8) | 79.2(4) | C(11)−W(4)−C(10) | 81.2(4) |
| C(11)−W(4)−C(12) | 80.3(4) | C(10)−W(4)−C(12) | 82.2(4) |
| S(2)−W(1)−S(1) | 106.52(9) | S(2)−W(1)−S(3) | 105.71(10) |
| S(1)−W(1)−S(3) | 102.17(9) | S(3)−W(2)−S(4) | 105.74(10) |
| S(3)−W(2)−S(1) | 102.70(9) | S(4)−W(2)−S(1) | 105.62(9) |
| S(1)−W(3)−S(2) | 106.49(9) | S(1)−W(3)−S(4) | 106.13(10) |
| S(2)−W(3)−S(4) | 101.83(10) | S(2)−W(4)−S(3) | 105.94(10) |
| S(2)−W(4)−S(4) | 102.25(9) | S(3)−W(4)−S(4) | 105.35(10) |
| W(1)−S(2)−W(4) | 72.64(8) | W(1)−S(2)−W(3) | 71.70(8) |
| W(4)−S(2)−W(3) | 74.65(8) | W(2)−S(3)−W(4) | 72.79(8) |
| W(2)−S(3)−W(1) | 74.17(8) | W(4)−S(3)−W(1) | 72.05(8) |
| W(2)−S(4)−W(3) | 72.02(8) | W(2)−S(4)−W(4) | 72.41(8) |
| W(3)−S(4)−W(4) | 74.30(8) | | |

**Table 3.** Selected Bond Lengths (Å) and Angles (deg) for **2**[a]

| | | | |
|---|---|---|---|
| W(1)−W(1A) | 2.886(2) | W(1)−W(2) | 2.887(1) |
| W(1)−W(2A) | 2.887(1) | W(2)−W(1A) | 2.887(1) |
| W(2)−W(2A) | 2.874(2) | W(1)−Se(1) | 2.507(2) |
| W(1)−Se(1A) | 2.507(2) | W(1)−Se(2) | 2.501(3) |
| W(2)−Se(1) | 2.507(3) | W(2)−Se(2) | 2.506(2) |
| W(2)−Se(2A) | 2.506(2) | W(1)−C(11) | 2.20(2) |
| W(1)−C(12) | 2.14(2) | W(1)−C(12B) | 2.14(2) |
| W(2)−C(21) | 2.08(3) | W(2)−C(22) | 2.11(2) |
| W(2)−C(22C) | 2.11(2) | | |
| Se(1A)−W(1)−Se(1) | 106.75(7) | Se(2)−W(1)−Se(1A) | 106.55(7) |
| Se(2)−W(1)−Se(1) | 106.55(7) | Se(2A)−W(2)−Se(1) | 106.40(7) |
| Se(2)−W(2)−Se(1) | 106.40(7) | Se(2A)−W(2)−Se(2) | 107.13(8) |
| C(12)−W(1)−C(11) | 80.8(6) | C(12B)−W(1)−C(11) | 80.8(6) |
| C(12)−W(1)−C(12B) | 80(1) | C(21)−W(2)−C(22) | 80.3(9) |
| C(21)−W(2)−C(22C) | 80.3(9) | C(22)−W(2)−C(22C) | 80(1) |
| W(1A)−Se(1)−W(1) | 70.26(7) | W(1A)−Se(1)−W(2) | 70.30(6) |
| W(1)−Se(1)−W(2) | 70.30(6) | W(1)−Se(2)−W(2A) | 70.42(7) |
| W(1)−Se(2)−W(2) | 70.42(7) | W(2A)−Se(2)−W(2) | 69.97(7) |

[a] Symmetry transformations used to generate equivalent atoms: A, $-x, -y + 1/2, z$; B, $-x, y, z$; C, $x, -y + 1/2, z$.

also been developed for molybdenum.[3,5,6] The $\beta$-$[W_4S_4(\mu\text{-dtp})_2(\text{dtp})_4]$ and α-$[W_4S_4(\mu\text{-dtp})_3(\text{dtp})_3]$ cuboidal $W_4S_4^{6+}$ core complexes have been obtained from $[W(CO)_6]$ and $Na_2[WO_4]$ or $K_3[W_2Cl_9]$ in the presence of $P_2S_5$ in ethanol.[23] Poor reproducibility and low yields are however noted in the latter case. Moreover many of the traditional reagents used in sulfide/selenide chemistry, e.g., $H_2E$ or $ME_4^{2-}$ (M = Mo, W; E = S, Se), cannot readily be used in the corresponding telluride chemistry.[7,39] As a result, methods of solution synthesis by self-assembly or fragment condensation have not been developed for $Mo_4Te_4$ and $W_4Te_4$ cubes. Cuboidal $M_4Te_4$ complexes are known for transition metals M = Mn, Re, Fe, Ru, Rh, Ir, Ni, and Pt, but with the exception of Fe these do not have as highly developed $M_4S_4$ and $M_4Se_4$ chemistry as in the case of Mo.[40]

Our recent efforts have therefore focused on the development of a high-temperature technique for the synthesis of polymeric solid-state molybdenum/tungsten chalcogenides as starting materials for the preparation of chalcogenide complexes.[32,41] Reactions of molybdenum and tungsten chalcogenides with $CN^-$ in aqueous solutions, and now in mixtures at high temperatures, are summarized in Scheme 1. Thus the tendency of $[M_3E_4$-

(38) McLean, I. J.; Hernandez-Molina, R.; Sokolov, M. N.; Seo, M.-S.; Virovets, A. V.; Elsegood, M. R. J.; Clegg, W.; Sykes, A. G. *J. Chem. Soc., Dalton Trans.* **1998**, 2557.

(39) Beck, J. *Angew. Chem., Int. Ed. Engl.* **1994**, *33*, 163.

(40) (a) $Mn_4Te_4$: Stephan, H.-O.; Henkel, G. *Angew. Chem., Int. Ed. Engl.* **1994**, *33*, 2322. (b) $Re_4Te_4$: Mironov, Y. V.; Albrecht-Schmitt, T. E.; Ibers, J. A. *Inorg. Chem.* **1997**, *36*, 944. (c) $Fe_4Te_4$: Stephan, H.-O.; Chen, C.; Henkel, G.; Griesar, K.; Haase, W. *J. Chem. Soc., Chem. Commun.* **1993**, 886. Barbaro, P.; Bencini, A.; Bertini, I.; Briganti, F.; Midollini, S. *J. Am. Chem. Soc.* **1990**, *112*, 7238. Steigerwald, M. L.; Siegrist, T.; Stuczynski, S. M.; Kwon, Y. U. *J. Am. Chem. Soc.* **1992**, *114*, 3155. Steigerwald, M. L.; Siegrist, T.; Gyorgy, E. M.; Hessen, B.; Kwon, Y.-U.; Tanzier, S. M. *Inorg. Chem.* **1994**, *33*, 3389. Stephan, H.-O.; Chen, C.; Henkel, G.; Griesar, K.; Haase, W. *J. Chem. Soc., Chem. Commun.* **1993**, 886. (d) $Ru_4Te_4$: Houser, E. J.; Rauchfuss, T. B.; Wilson, S. R. *Inorg. Chem.* **1993**, *32*, 4069. (e) $Rh_4Te_4$: Schulz, S.; Andruh, M.; Pape, T.; Heinze, T.; Roesky, H. W.; Haming, L.; Kuhn, A.; Herbst-Irmer, R. *Organometallics* **1994**, *13*, 4004. (f) $Ir_4Te_4$: Schulz, S.; Andruh, M.; Pape, T.; Heinze, T.; Roesky, H. W.; Haming, L.; Kuhn, A.; Herbst-Irmer, R. *Organometallics* **1994**, *13*, 4004. (g) $Ni_4Te_4$: McConnachie, J. M.; Ansari, M. A.; Ibers, J. A. *Inorg. Chim. Acta* **1992**, *198*−*200*, 85. McConnachie, J. M.; Bollinger, J. S.; Ibers, J. A. *Inorg. Chem.* **1993**, *32*, 3923. (h) $Pt_4Te_4$: McConnachie, J. M.; Bollinger, J. C.; Ibers, J. A. *Inorg. Chem.* **1993**, *32*, 3923.

**Table 4.** Selected Bond Lengths (Å) and Angles (deg) for **3**

| | | | |
|---|---|---|---|
| W(1)−W(2) | 2.957(1) | W(1)−W(3) | 2.923(1) |
| W(1)−W(4) | 2.839(1) | W(2)−W(3) | 3.054(1) |
| W(2)−W(4) | 3.008(1) | W(3)−W(4) | 2.991(2) |
| W(1)−Te(1) | 2.702(2) | W(1)−Te(2) | 2.686(2) |
| W(1)−Te(3) | 2.704(2) | W(2)−Te(1) | 2.677(2) |
| W(2)−Te(3) | 2.679(2) | W(2)−Te(4) | 2.674(2) |
| W(3)−Te(2) | 2.677(2) | W(3)−Te(3) | 2.678(2) |
| W(3)−Te(4) | 2.680(2) | W(4)−Te(1) | 2.682(2) |
| W(4)−Te(2) | 2.697(2) | W(4)−Te(4) | 2.700(2) |
| W(1)−C(11) | 2.12(2) | W(1)−C(12) | 2.13(2) |
| W(1)−C(13) | 2.20(3) | W(2)−C(21) | 2.16(3) |
| W(2)−C(22) | 2.14(2) | W(2)−C(23) | 2.12(2) |
| W(3)−C(31) | 2.14(3) | W(3)−C(32) | 2.20(3) |
| W(3)−C(33) | 2.16(3) | W(4)−C(41) | 2.16(2) |
| W(4)−C(42) | 2.10(3) | W(4)−C(43) | 2.17(3) |
| Te(1)−W(1)−Te(3) | 108.18(6) | Te(2)−W(1)−Te(1) | 112.44(6) |
| Te(2)−W(1)−Te(3) | 109.14(6) | Te(1)−W(2)−Te(3) | 109.68(6) |
| Te(4)−W(2)−Te(1) | 107.95(6) | Te(4)−W(2)−Te(3) | 106.49(6) |
| Te(2)−W(3)−Te(3) | 110.22(6) | Te(2)−W(3)−Te(4) | 108.62(6) |
| Te(3)−W(3)−Te(4) | 106.38(6) | Te(1)−W(4)−Te(2) | 112.71(6) |
| Te(1)−W(4)−Te(4) | 107.03(6) | Te(2)−W(4)−Te(4) | 107.41(6) |
| C(11)−W(1)−C(12) | 82(1) | C(11)−W(1)−C(13) | 80.0(9) |
| C(12)−W(1)−C(13) | 82.6(8) | C(22)−W(2)−C(21) | 81(1) |
| C(23)−W(2)−C(21) | 78.6(9) | C(23)−W(2)−C(22) | 81(1) |
| C(31)−W(3)−C(32) | 79(1) | C(31)−W(3)−C(33) | 78(1) |
| C(33)−W(3)−C(32) | 79(1) | C(41)−W(4)−C(43) | 80(1) |
| C(42)−W(4)−C(41) | 80.5(9) | C(42)−W(4)−C(43) | 83(1) |
| W(2)−Te(1)−W(1) | 66.70(5) | W(2)−Te(1)−W(4) | 68.28(5) |
| W(4)−Te(1)−W(1) | 63.65(5) | W(1)−Te(2)−W(4) | 63.67(4) |
| W(3)−Te(2)−W(1) | 66.06(5) | W(3)−Te(2)−W(4) | 67.65(5) |
| W(2)−Te(3)−W(1) | 66.64(5) | W(3)−Te(3)−W(1) | 65.79(5) |
| W(3)−Te(3)−W(2) | 69.52(5) | W(2)−Te(4)−W(3) | 69.57(5) |
| W(2)−Te(4)−W(4) | 68.06(5) | W(3)−Te(4)−W(4) | 67.56(5) |

$(CN)_9]^{5-}$ (M = Mo, W; E = S, Se) complexes to form on reaction of polymeric chain compounds $\{M_3E_7Br_4\}_x$ with aqueous solutions of $CN^-$ has been demonstrated.[42] In these reactions, abstraction of S or Se from bridging $\mu$-$E_2$ ligands of the starting compounds is observed.[43] In contrast, no similar abstraction is observed in the reaction of $\{Mo_3Te_7I_4\}_x$ with aqueous $CN^-$, and instead the triangular $[Mo_3Te_7(CN)_6]^{2-}$ complex is obtained in high yield.[32] For the preparation of the chalcogenide cuboidal complexes, Figure 1, we have used high-temperature reactions with KCN at 430−450 °C (note that the melting point of KCN is 635 °C). Dark red-brown crystals of the telluride complexes $K_7[Mo_4(\mu_3\text{-}Te)_4(CN)_{12}]\cdot 12H_2O$ (**5**) and $K_6[W_4(\mu_3\text{-}Te)_4(CN)_{12}]\cdot 5H_2O$ (**3**) were obtained in high yields (>80%) by the high-temperature reaction of $\{Mo_3Te_7I_4\}_x$ or $WTe_2$ with $CN^-$ at 450 °C and further crystallization from aqueous solutions. The higher charge on the $W_4Te_4$ cluster is consistent with the greater difficulty in reducing W to its lower oxidation states. Cyanotungstates **1** and **2** were obtained in moderate yields. In these cases formation of stable $WS_2$ and $WSe_2$ was demonstrated by powder diffraction data. The oxidized form $Cs_6[Mo_4(\mu_3\text{-}Te)_4(CN)_{12}]\cdot 2H_2O$ (**4**) was prepared by the oxidation of $K_7[Mo_4(\mu_3\text{-}Te)_4(CN)_{12}]\cdot 12H_2O$ (**5**) with bromine water at room temperature.

$$[Mo_4Te_4(CN)_{12}]^{7-} + {}^1/_2Br_2 \rightarrow [Mo_4Te_4(CN)_{12}]^{6-} + Br^-$$

The high-temperature reaction of $WTe_2$ with $SCN^-$ gives $K_6[W_4(\mu_3\text{-}S)_4(CN)_{12}]\cdot 4H_2O$, with no evidence for formation of mixed S/Te cuboidal complexes.

The cluster compounds **1**−**5** are stable indefinitely in air at 95 °C in aqueous solutions (pH 2−10), with no tendency to lose core atoms.

**Molecular and Crystal Structures.** The cluster anions shown in Figures 2−5 have similar structures. The metal and chalcogen atoms form a distorted cube, and in addition each metal is coordinated by three practically linear CN groups. The following conclusions can be made from the main geometrical characteristics of $M_4E_4$ cores listed in Table 7. First, all the $M_4$ tetrahedra except that of $W_4$ in **2** are to some extent distorted, with M−M bond lengths showing significant variations. At the same time distortions of pyramidal $M_3E$ as measured by $\Delta$(M−E) are less. Such distortions can be brought about in many ways including electronic properties of cluster anions, their crystallographic environment, and cation−anion and anion−water molecule interactions. The comparison of $M_4$ and $M_3E$ distortions leads to the conclusion that M−M bonds for any one cube are more variable and less rigid than M−E bonds. The M−E distances vary regularly in the sequence W−S < W−Se < W−Te. The W−W bond lengths and volumes of $W_4$ tetrahedra decrease systematically in going from **3** to **2** to **1**, with the mean Mo−Mo bond length in **4** only 0.004 Å less than that for W−W in **3**.

The cluster anions in **4** and **5** differ in the mean oxidation state of the molybdenum atoms. The anion in **5** may be considered as the product of one-electron reduction of **4**. It causes the following changes in the geometry of the cluster cores: the mean Mo−Mo bond length and volume of the $Mo_4$ tetrahedron increase, and the distortion of the $Mo_4$ tetrahedron decreases. The mean Mo−Te bond length increases in going from **4** to **5** (0.026 Å). It is of interest that Shibahara et al. noted a decrease in Mo−Mo bond lengths and volumes of $Mo_4$ tetrahedra on reduction of the $Mo_4S_4$ core in $[Mo_4S_4(edta)_2]^{n-}$ ($n$ = 2,3,4).[44] At the same time the Mo−S bonds show little change as in our case. The different dimensions of the $Mo_4Te_4$ and $Mo_4S_4$ cores requires further investigation.

From the crystallographic point of view an interesting problem is the influence of crystal packing on the geometry of $M_4E_4$ cluster cores. Such interactions may be responsible for the discrepancy between X-ray diffraction and NMR data (see below) concerning the equivalence or nonequivalence of metal atoms. The most interesting crystal packing is in the case of compound **4**. First, the space group $P2_1$ is chiral and polar, and the compound may therefore possess polar solid-state properties such as pyroelectricity. Polar structures are unusual for crystals composed of nonchiral cations and anions. It is important to keep in mind that the chirality of the crystal structure of **4** means not only the chirality of the cluster anions whose cores are slightly distorted but also the chirality of whole cation−anion packing. This is why we have not tried to examine the absolute configuration of **4**; such an examination would reveal the "sign" of $Cs^+$ packing together with the "sign" of the cluster anions in individual crystals.

Another interesting feature of crystal packing of **4** is that it is composed from heavy scattering cations and anions. Following the approach proposed by Borisov et al.,[45] the heavy structural moieties are located in the planes perpendicular to the *b* axis (Figure 6). In this case, the crystallographic *y* coordinates of the sections which involve Mo, Te, and Cs atoms of two moieties (linked by the $2_1$ screw axis) differ by no more than 0.05. We believe that this is a possible factor affecting the quality of single crystals; small differences in the Mo and Cs (or Cs and Te) plane coordinates provide a means of creating

(41) Fedin, V. P.; Imoto, H.; Saito, T. *J. Chem. Soc., Chem. Commun*. **1995**, 1559.
(42) Fedin, V. P.; Lamprecht, G. J.; Kohzuma, T.; Clegg, W.; Elsegood, M. R. J.; Sykes, A. G. *J. Chem. Soc., Dalton Trans*. **1997**, 1747.
(43) Saysell, D. M.; Fedin, V. P.; Lamprecht, G. R.; Sokolov, M. N.; Sykes, A. G. *Inorg. Chem*. **1997**, *36*, 2982.
(44) Shibahara, T.; Akashi, H.; Matsumoto, K.; Ooi, S. *Inorg. Chim. Acta* **1993**, *212*, 251.
(45) Borisov, S. V.; Podberezskaya, N. V.; Pervukhina, N. V.; Magarill, S. A. *Z. Kristallogr*. **1998**, *B213*, 1.

**Scheme 1.** Summary of Reactions of Molybdenum and Tungsten Chalcogenides with $CN^-$

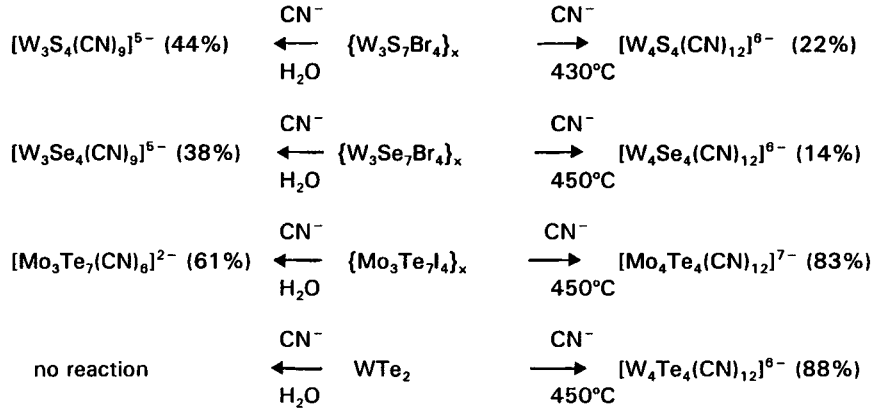


**Table 5.** Selected Bond Lengths (Å) and Angles (deg) for **4**

| | | | |
|---|---|---|---|
| Mo(1)−Mo(2) | 3.016(7) | Mo(1)−Mo(3) | 2.932(6) |
| Mo(1)−Mo(4) | 3.055(6) | Mo(2)−Mo(3) | 2.860(5) |
| Mo(2)−Mo(4) | 3.016(6) | Mo(3)−Mo(4) | 2.916(6) |
| Te(1)−Mo(1) | 2.671(5) | Te(1)−Mo(2) | 2.671(5) |
| Te(1)−Mo(3) | 2.689(5) | Te(2)−Mo(1) | 2.656(5) |
| Te(2)−Mo(2) | 2.684(6) | Te(2)−Mo(4) | 2.674(5) |
| Te(3)−Mo(2) | 2.694(6) | Te(3)−Mo(3) | 2.691(6) |
| Te(3)−Mo(4) | 2.672(6) | Te(4)−Mo(1) | 2.664(5) |
| Te(4)−Mo(3) | 2.701(6) | Te(4)−Mo(4) | 2.670(5) |
| Mo(1)−C(11) | 2.08(5) | Mo(1)−C(12) | 2.10(5) |
| Mo(1)−C(13) | 2.10(5) | Mo(2)−C(21) | 2.14(6) |
| Mo(2)−C(22) | 2.21(5) | Mo(2)−C(23) | 2.06(4) |
| Mo(3)−C(31) | 2.23(6) | Mo(3)−C(32) | 2.23(6) |
| Mo(3)−C(33) | 2.19(7) | Mo(4)−C(41) | 2.16(6) |
| Mo(4)−C(42) | 2.15(5) | Mo(4)−C(43) | 2.16(5) |
| Te(2)−Mo(1)−Te(1) | 107.5(2) | Te(2)−Mo(1)−Te(4) | 106.3(2) |
| Te(4)−Mo(1)−Te(1) | 110.4(2) | Te(1)−Mo(2)−Te(2) | 106.7(2) |
| Te(1)−Mo(2)−Te(3) | 112.1(2) | Te(2)−Mo(2)−Te(3) | 107.0(2) |
| Te(1)−Mo(3)−Te(4) | 108.7(2) | Te(3)−Mo(3)−Te(1) | 111.6(2) |
| Te(3)−Mo(3)−Te(4) | 109.3(2) | Te(3)−Mo(4)−Te(2) | 107.9(2) |
| Te(4)−Mo(4)−Te(2) | 105.6(2) | Te(4)−Mo(4)−Te(3) | 110.8(2) |
| C(11)−Mo(1)−C(12) | 78(2) | C(13)−Mo(1)−C(11) | 77(2) |
| C(13)−Mo(1)−C(12) | 81(2) | C(21)−Mo(2)−C(22) | 83(2) |
| C(23)−Mo(2)−C(21) | 84(2) | C(23)−Mo(2)−C(22) | 81(2) |
| C(31)−Mo(3)−C(32) | 82(2) | C(33)−Mo(3)−C(31) | 83(2) |
| C(33)−Mo(3)−C(32) | 77(2) | C(42)−Mo(4)−C(41) | 79(2) |
| C(42)−Mo(4)−C(43) | 80(2) | C(43)−Mo(4)−C(41) | 78(2) |
| Mo(1)−Te(1)−Mo(3) | 66.3(2) | Mo(2)−Te(1)−Mo(1) | 68.8(2) |
| Mo(2)−Te(1)−Mo(3) | 64.5(1) | Mo(1)−Te(2)−Mo(2) | 68.8(2) |
| Mo(1)−Te(2)−Mo(4) | 70.0(2) | Mo(4)−Te(2)−Mo(2) | 68.5(2) |
| Mo(3)−Te(3)−Mo(2) | 64.2(1) | Mo(4)−Te(3)−Mo(2) | 68.4(2) |
| Mo(4)−Te(3)−Mo(3) | 65.9(2) | Mo(1)−Te(4)−Mo(3) | 66.2(2) |
| Mo(1)−Te(4)−Mo(4) | 69.9(2) | Mo(4)−Te(4)−Mo(3) | 65.8(2) |

**Table 6.** Selected Bond Lengths (Å) and Angles (deg) for **5**[a]

| | | | |
|---|---|---|---|
| Mo(1)−Mo(2) | 3.0013(9) | Mo(1)−Mo(2A) | 3.0013(9) |
| Mo(1)−Mo(3) | 2.980(1) | Mo(2)−Mo(2A) | 2.967(1) |
| Mo(2)−Mo(3) | 3.002(1) | Mo(3)−Mo(2A) | 3.002(1) |
| Te(1)−Mo(1) | 2.6663(7) | Te(1)−Mo(2) | 2.6663(8) |
| Te(1)−Mo(3) | 2.6747(7) | Te(2)−Mo(1) | 2.686(1) |
| Te(2)−Mo(2) | 2.6717(8) | Te(2)−Mo(2A) | 2.6717(8) |
| Te(3)−Mo(2) | 2.6763(8) | Te(3)−Mo(2A) | 2.6763(8) |
| Te(3)−Mo(3) | 2.674(1) | Mo(1)−C(11) | 2.151(8) |
| Mo(1)−C(11A) | 2.151(8) | Mo(1)−C(12) | 2.16(1) |
| Mo(2)−C(21) | 2.171(8) | Mo(2)−C(22) | 2.168(8) |
| Mo(2)−C(23) | 2.162(8) | Mo(3)−C(31) | 2.176(8) |
| Mo(3)−C(31A) | 2.176(8) | Mo(3)−C(32) | 2.15(1) |
| Te(1A)−Mo(1)−Te(1) | 109.20(4) | Te(1A)−Mo(1)−Te(2) | 107.40(2) |
| Te(1)−Mo(1)−Te(2) | 107.40(2) | Te(1)−Mo(2)−Te(2) | 107.82(3) |
| Te(1)−Mo(2)−Te(3) | 107.72(3) | Te(2)−Mo(2)−Te(3) | 109.16(3) |
| Te(1A)−Mo(3)−Te(1) | 108.69(4) | Te(3)−Mo(3)−Te(1A) | 107.55(2) |
| Te(3)−Mo(3)−Te(1) | 107.55(2) | C(11A)−Mo(1)−C(11) | 80.0(5) |
| C(11A)−Mo(1)−C(12) | 79.9(3) | C(11)−Mo(1)−C(12) | 79.9(3) |
| C(21)−Mo(2)−C(22) | 81.6(3) | C(23)−Mo(2)−C(21) | 80.3(3) |
| C(23)−Mo(2)−C(22) | 80.2(3) | C(31A)−Mo(3)−C(31) | 79.5(4) |
| C(32)−Mo(3)−C(31A) | 80.4(3) | C(32)−Mo(3)−C(31) | 80.4(3) |
| Mo(1)−Te(1)−Mo(3) | 67.83(3) | Mo(2)−Te(1)−Mo(1) | 68.50(2) |
| Mo(2)−Te(1)−Mo(3) | 68.40(3) | Mo(2A)−Te(2)−Mo(1) | 68.14(2) |
| Mo(2)−Te(2)−Mo(1) | 68.14(2) | Mo(2A)−Te(2)−Mo(2) | 67.46(3) |
| Mo(2A)−Te(3)−Mo(2) | 67.33(3) | Mo(3)−Te(3)−Mo(2A) | 68.27(2) |
| Mo(3)−Te(3)−Mo(2) | 68.27(2) | | |

[a] Symmetry transformations used to generate equivalent atoms: A, $x, -y + 3/2, z$.

a crystallographic shift into the other plane resulting in a reduction in symmetry and hence in crystal quality.

The centers of cluster anions are stacked by the pseudohexagonal law forming layers in the (101) plane (Figure 7).

**NMR Spectra.** The spin $1/2$ isotopes $^{77}$Se, $^{125}$Te, and $^{183}$W provide a valuable tool in NMR spectroscopy for the characterization of the tungsten−chalcogen complexes. The $^{125}$Te and $^{183}$W spectra obtained for **3** are given as examples in Figure 8. The $^{77}$Se, $^{125}$Te and $^{183}$W NMR chemical shifts and $^1$J(W−E) (E = Se, Te) observed, are summarized in Table 8. Spectra measured at room temperature give singlets with satellite lines. The spectra are in good agreement with those calculated on the basis of the natural abundance of isotopes $^{77}$Se (7.58%), $^{125}$Te (6.99%), and $^{183}$W (14.40%). According to the X-ray structure analysis, distortions from ideal $T_d$ symmetry do occur for the mixed-valance complexes **1**−**3**. The NMR spectra demonstrate unambiguously identical environments for W and E atoms in aqueous solution studies. The NMR results are in excellent agreement with the X-ray crystallography results, which indicate four equivalent W atoms each coordinated by three triply bridging chalcogen atoms in $[W_4E_4(CN)_{12}]^{6-}$. We propose that the cluster symmetry in solution is effectively increased by rapid dynamic processes. A stereochemical nonrigidity has been demonstrated for the mixed-valent $[(MeC_5H_4)_4Ru_4E_4]^{2+}$ complexes.[46]

The chemical shift of W in $[W_4S_4(CN)_{12}]^{6-}$ is shifted downfield 633 and 1753 ppm, relative to the chemical shifts of W in $[W_4Se_4(CN)_{12}]^{6-}$ and $[W_4Te_4(CN)_{12}]^{6-}$, respectively. The wide range of chemical shifts and the coupling information available from the observation of satellite peaks has demonstrated the usefulness of the NMR technique. The review by Ansari and Ibers contains tabulated data of known chemical shifts, and coupling constants for metal selenides and tellurides have been reported.[47] Additional data are needed so that the scale for $^{77}$Se and $^{125}$Te NMR chemical shifts can be established.

(46) Houser, E. J.; Rauchfuss, T. B.; Wilson, S. R. *Inorg. Chem.* **1993**, *32*, 4069.

(47) Ansari, M. A.; Ibers, J. A. *Coord. Chem. Rev.* **1990**, *90*, 223. See also: Bollinger, J. C.; Ibers, J. A. *Inorg. Chem.* **1995**, *34*, 1859. Compton, N. A.; Errington, R. J.; Norman, N. C. *Adv. Organomet. Chem.* **1990**, *31*, 91.

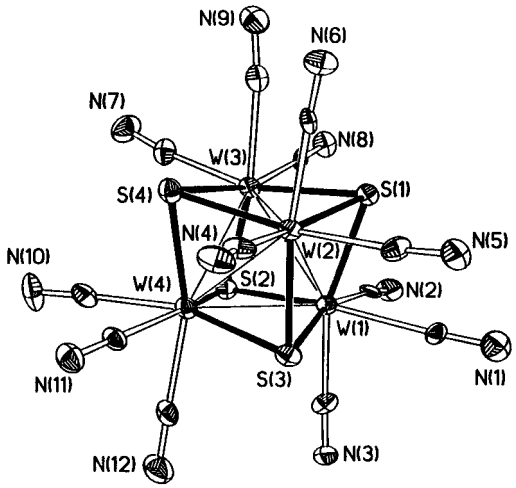


**Figure 2.** Anion $[W_4S_4(CN)_{12}]^{6-}$ in **1**. In Figures 2−5, ellipsoids are at the 50% probability level, and M−M bonds are shown as thin lines, M−E solid, and M−C open. Unique atoms are labeled except for C atoms, which have the same number as the corresponding N atoms in each case.

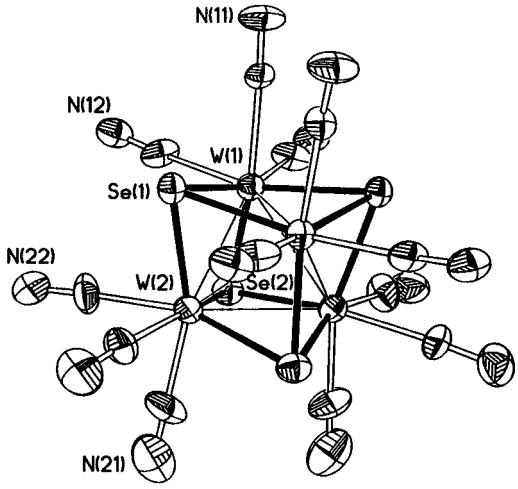


**Figure 3.** Anion $[W_4Se_4(CN)_{12}]^{6-}$ in **2**.

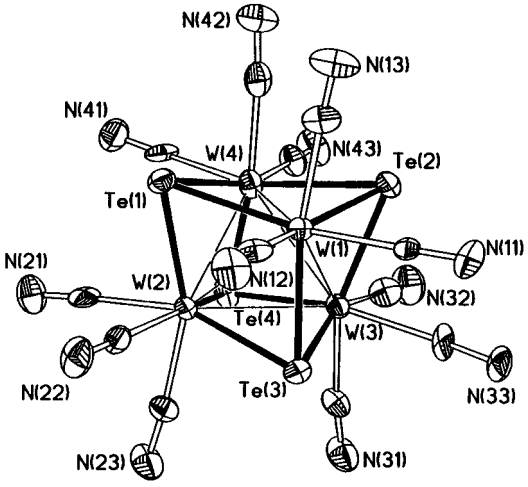


**Figure 4.** Anion $[W_4Te_4(CN)_{12}]^{6-}$ in **3**. The anion $[Mo_4Te_4(CN)_{12}]^{6-}$ in **4** is almost identical, with the same numbering scheme.

Solutions of diamagnetic complexes **1**−**3** were found to be stable for extended periods of time at 20 °C and gave virtually unchanged NMR spectra over several months.

**IR Spectra.** Spectra of **1**−**5** in KBr and Nujol are identical. Intense bands due to $H_2O$ absorption at 3600−3200 $cm^{-1}$ (antisymmetric and symmetric stretches) and at ∼1600 $cm^{-1}$ ($\delta$ HOH) were observed for compounds **1**−**5**. The $\nu$(CN) frequencies for compounds **1**−**5** are listed in Table 9. Cyano complexes can be identified easily since they exhibit $\nu$(CN) at ∼2100 $cm^{-1}$. Only single sharp bands were observed for the mixed-valent complexes **1**−**5**. The $\nu$(CN) of free $CN^-$ is 2080 $cm^{-1}$. Upon coordination the $\nu$(CN) shifts to higher frequencies.[48] The $CN^-$ ion acts as $\sigma$-donor, with some $\pi$-acceptor M → $\pi^*$(CN) back-bonding. The $\nu$(CN) frequencies of the molybdenum and tungsten complexes are dependent on the chalcogen and oxidation state of the metal. The effect of the chalcogen is in the order

$$\mathbf{1}\ (2125\ cm^{-1}) > \mathbf{2}\ (2116\ cm^{-1}) > \mathbf{3}\ (2097\ cm^{-1})$$

The effect of oxidation state is seen in the frequency order for two molybdenum complexes:

$$\mathbf{5}\ (2086\ cm^{-1}) < \mathbf{4}\ (2102\ cm^{-1})$$

With an increasing number of (formal) molybdenum electrons, the Mo → $\pi^*$(CN) back-bonding becomes more important.

In addition to $\nu$(CN), the cyano complexes exhibit $\nu$(MC)/$\delta$(MoCN) bands in the low-frequency region (400−430 $cm^{-1}$) (Table 9). Normal coordinate analyses have been carried out on the cyano complexes.[46] For tetranuclear $[Mo_4S_4(CN)_{12}]^{8-}$ it has been shown that the $\nu$(MC) and $\delta$(MoCN) vibrations appear in the region >370 $cm^{-1}$.

**UV−Vis Spectra.** SCCC-EH-MO calculations have been carried out on $[Mo_4S_4(CN)_{12}]^{8-}$.[49] The calculations show that MOs, which are responsible for the bonding within the central $Mo_4S_4$ fragment, are rather localized. In the HOMO/LUMO region there are six bonding orbitals ($a_1$, e, $t_2$; occupied in the complex) and six antibonding orbitals ($t_1$, $t_2$; unoccupied), which have mainly Mo 4d character. Peak positions and intensities of the bands in UV−vis spectra of compounds **1**−**5** (Figures 9 and 10) are comparable to those of $Mo_4S_4$ and $Mo_4Se_4$ systems. Absorption around 40 000 $cm^{-1}$ (with $\epsilon$ values of ca. $10^4$ $M^{-1}cm^{-1}$) in all complexes (as in simpler mononuclear octacyanomolybdates and -tungstates) are assigned to CN → M (M = Mo, W) charge-transfer transitions.[50] The lower energy

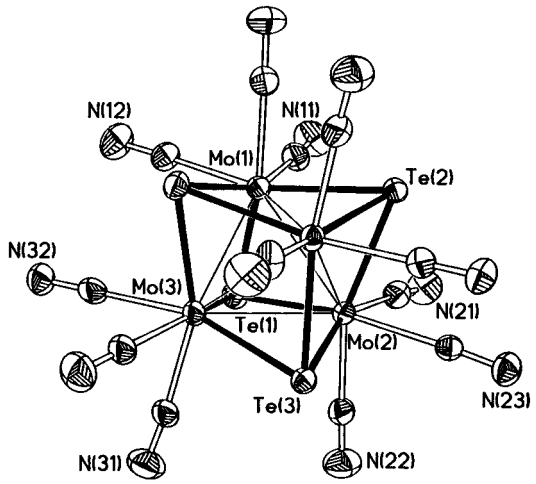


**Figure 5.** Anion $[Mo_4Te_4(CN)_{12}]^{7-}$ in **5**.

(48) Nakamoto, K. *Infrared and Raman Spectra of Inorganic and Coordination Compounds*, 3rd ed.; Wiley: New York, 1978.
(49) Müller, A.; Jostes, R.; Eltzner, W.; Nie, C.-S.; Diemann, E.; Bögge, H.; Zimmermann, M.; Dartmann, M.; Reinsh-Vogell, U.; Che, S.; Cyvin, S. J.; Cyvin, B. N. *Inorg. Chem.* **1985**, *24*, 2872.
(50) Golebiewski, A.; Kowalski, H. *Theor. Chim. Acta* **1968**, *12*, 293.

**Table 7.** Some Geometrical Characteristics of $M_4E_4$ Cluster Cores

| | $Cs_5K[W_4S_4(CN)_{12}]\cdot CH_3OH\cdot 2H_2O$ (**1**) | $K_6[W_4Se_4(CN)_{12}]\cdot 6H_2O$ (**2**) | $K_6[W_4Te_4(CN)_{12}]\cdot 5H_2O$ (**3**) | $Cs_6[Mo_4Te_4(CN)_{12}]\cdot 2H_2O$ (**4**) | $K_7[Mo_4Te_4(CN)_{12}]\cdot 12H_2O$ (**5**) |
|---|---|---|---|---|---|
| oxidation state of M | 3.5 | 3.5 | 3.5 | 3.5 | 3.25 |
| crystallographic symmetry of cluster | $C_1$ | $C_{2v}$ | $C_1$ | $C_1$ | $C_s$ |
| vol of $M_4$, Å$^3$ | 2.710 | 2.828 | 3.055 | 3.067 | 3.157 |
| M−M mean, Å | 2.845 | 2.884 | 2.962 | 2.966 | 2.992 |
| Δ(M−M) with esd, Å | 0.104(1) | 0.013(1) | 0.215(2) | 0.195(6) | 0.035(1) |
| M−E mean, Å | 2.394 | 2.506 | 2.686 | 2.678 | 2.674 |
| Δ(M−E) with esd, Å | 0.006(1) | 0.006(3) | 0.030(2) | 0.045(6) | 0.020(1) |

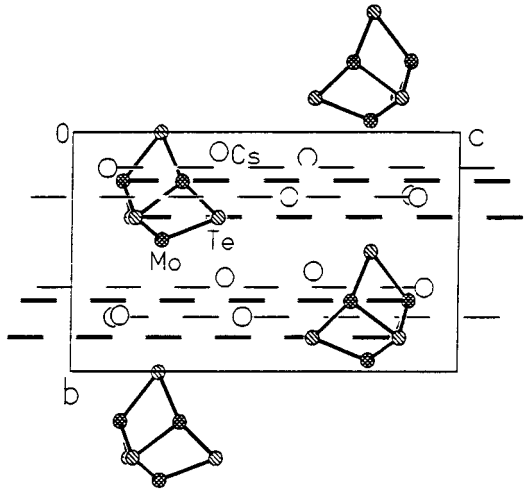


**Figure 6.** Crystal packing in compound **5** (projection along the *x* axis). Only $Mo_4Te_4$ cluster cores and $Cs^+$ cations are shown for clarity. The traces of Mo, Te, and Cs planes are shown in dashed lines.

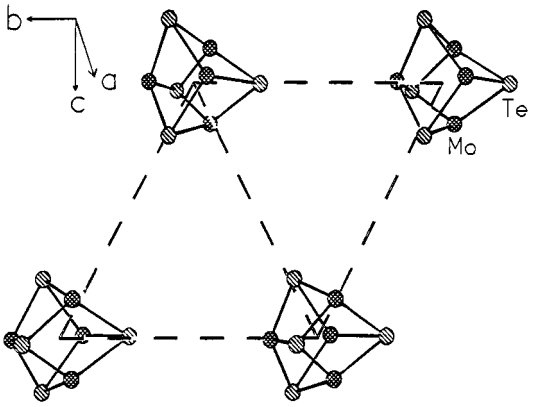


**Figure 7.** Fragment of the pseudohexagonal net of cluster anion centroids in compound **5** in projection on the (101) plane. Only $Mo_4Te_4$ cores are shown for clarity. The distances between centroids of 10.124 and 10.918 Å are shown as dashed lines. The angle at the apex of the isosceles triangle is 55.2°, and the angle at the base of the triangle is 62.4°.

transitions (in the near-IR/vis region) take place mainly within the $M_4E_4$ chromophore.

The lower energy peaks in the visible region for complexes **1**−**5** are dependent on the chalcogen, the metal atoms present, and the oxidation state of the metal atoms. The effect of the chalcogen and metal atoms is seen in the order

**1** (786 nm) < **2** (850 nm) < **3** (869 nm) < **4** (947 nm)

The effect of oxidation state is seen in the order

**5** (769 nm) < **4** (947 nm)

Red shifts in the UV−vis spectra have been observed on

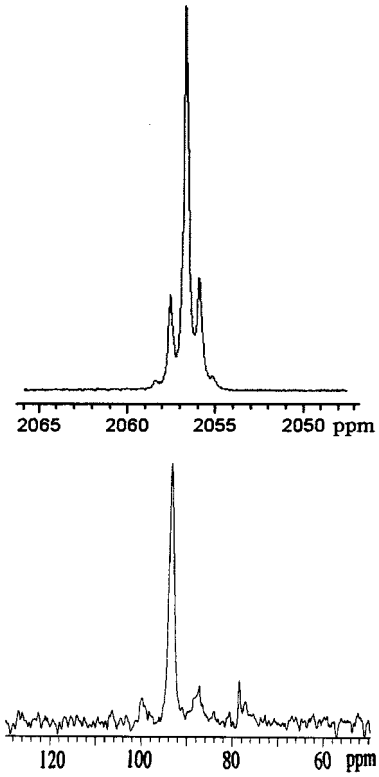


**Figure 8.** (a) $^{125}$Te and (b) $^{183}$W spectra of $K_6[W_4Te_4(CN)_{12}]\cdot 5H_2O$ (**3**) (0.266 M solution in $H_2$ at 293 K).

**Table 8.** Chemical Shifts and $J_{W-E}$ in NMR Spectra of Complexes **1**−**3** in Aqueous Solutions at 293 K

| complex | δ, ppm $^{183}$W | δ, ppm $^{77}$Se/$^{125}$Te | $J_{W-E}$, Hz |
|---|---|---|---|
| $[W_4S_4(CN)_{12}]^{6-}$ (**1**) | −1659 | | |
| $[W_4Se_4(CN)_{12}]^{6-}$ (**2**) | −1026 | 1496 | 55 |
| $[W_4Te_4(CN)_{12}]^{6-}$ (**3**) | 94 | 2061 | 156 |

**Table 9.** Selected Infrared Spectral Data of **1**−**5**

| complex | electron config for $M_4$ | ν(CN), cm$^{-1}$ | ν(MC) /δ(MoCN), cm$^{-1}$ |
|---|---|---|---|
| $KCs_5[W_4S_4(CN)_{12}]\cdot CH_3OH\cdot 2H_2O$ (**1**) | $(d^3)_2(d^2)_2$ | 2125 | 410 |
| $K_6[W_4Se_4(CN)_{12}]\cdot 6H_2O$ (**2**) | $(d^3)_2(d^2)_2$ | 2116 | 420 |
| $K_6[W_4Te_4(CN)_{12}]\cdot 5H_2O$ (**3**) | $(d^3)_2(d^2)_2$ | 2097 | 426 |
| $Cs_6[Mo_4Te_4(CN)_{12}]\cdot 2H_2O$ (**4**) | $(d^3)_2(d^2)_2$ | 2102 | 403 |
| $K_7[Mo_4Te_4(CN)_{12}]\cdot 12H_2O$ (**5**) | $(d^3)_3(d^2)$ | 2086 | 425 |

replacing Mo with W, and Se with S in trinuclear cyano complexes $[M_3E_4(CN)_9]^{5-}$ and in $[M_4E_4(H_2O)_{12}]^{5+}$.[17,18,42]

**Electrochemical Studies.** The cuboidal clusters $M_4S_4^{n+}$ (M = Fe, Mo) were the first clusters shown to display consecutive reversible multistep redox interconversions, a maximum of five

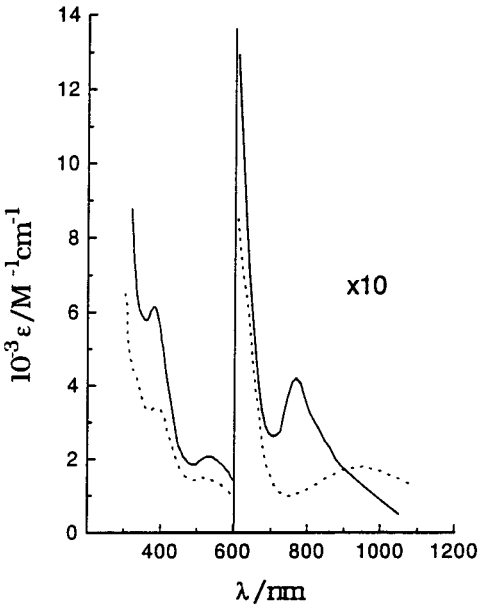


**Figure 9.** UV−vis spectra of $K_7[Mo_4Te_4(CN)_{12}]\cdot 12H_2O$ (**5**) (—) and $Cs_6[Mo_4Te_4(CN)_{12}]\cdot 2H_2O$ (**4**) (···) in $H_2O$.

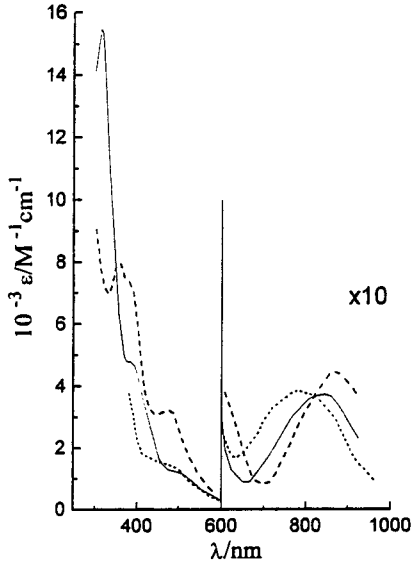


**Figure 10.** UV−vis spectra of $KCs_5[W_4S_4(CN)_{12}]\cdot CH_3OH\cdot 2H_2O$ (**1**) (···), $K_6[W_4Se_4(CN)_{12}]\cdot 6H_2O$ (**2**) (—), and $K_6[W_4Te_4(CN)_{12}]\cdot 5H_2O$ (**3**) (− − −) in $H_2O$.

(*n* from 0 to 4) for Fe and three (*n* from 4 to 6) for Mo.[49,51] Later, Se-substituted cubes prepared for both Fe and Mo were shown to display the same pattern of reversible multistep redox changes.[17] Our present results show that corresponding $W_4E_4^{n+}$ (E = S, Se, Te) cubes are also capable of existing in three oxidation states ranging from the most oxidized ($n = 6$; 10 electrons) to the most reduced electron-precise 12-electron species with $n = 4$. CV data for tungsten and molybdenum cyano complexes are summarized in Table 10. Figure 11 displays (as an example) the cyclic voltammogram of **3** in 0.10 M $Na_2SO_4$. Bridging by the increasingly heavier chalcogen (on going from S to Te) lowers the oxidation potential, thus making the electron-deficient 6+ state more stable, and decreases the stability of the electron-precise $M_4E_4^{4+}$ state. Similar trends are observed for heterometallic $[W_3MoE_4(H_2O)_{12}]^{4+}$ (E = S, Se).[38]

(51) Ferguson, J. A.; Meyer, T. J. *J. Chem. Soc., Chem. Commun*. **1971**, 623.

**Table 10.** Summary of CV Data (Potentials in mV Were Converted vs NHE; 25 °C) for **1**−**4** in Aqueous Solution (0.10 M $Na_2SO_4$)

| | $[W_4E_4]^{6+}/[W_4E_4]^{5+}$ | | | $[W_4E_4]^{5+}/[W_4E_4]^{4+}$ | | |
|---|---|---|---|---|---|---|
| complex | $E_a$ | $E_c$ | $E_{1/2}$ | $E_a$ | $E_c$ | $E_{1/2}$ |
| $[W_4S_4(CN)_{12}]^{6-}$ (**1**) | 807 | 735 | 769[a] | −277 | −329 | −299 |
| $[W_4Se_4(CN)_{12}]^{6-}$ (**2**) | 732 | 655 | 694[b] | −315 | −370 | −343 |
| $[W_4Te_4(CN)_{12}]^{6-}$ (**3**) | 589 | 513 | 559[c] | −366 | −428 | −397 |
| $[Mo_4Te_4(CN)_{12}]^{6-}$ (**4**) | 843 | 777 | 810[d] | 1 | −61 | −30 |

[a] $I_a/I_c = 1.4$. [b] $I_a/I_c = 1.3$ (25 mV/s), 1.6 (100 mV/s). [c] $I_a/I_c = 1.2$. [d] $I_a/I_c = 2.1$.

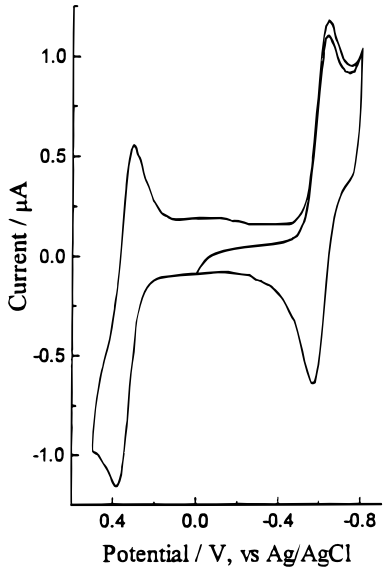


**Figure 11.** Cyclic voltammogram of $K_6[W_4Te_4(CN)_{12}]\cdot 5H_2O$ (**3**) in 0.1 M $Na_2SO_4$ at scan rate 100 mV $s^{-1}$.

At first sight, the trend is in keeping with decreasing electronegativity and increasing polarizability of the S−Se−Te series. However, the MO treatment of $Mo_4S_4$ clusters shows that in the process of oxidation of the cluster core from 4+ to 6+ electrons are taken from the $t_2$ MO (HOMO) with a predominantly 4d Mo character so that the influence of the bridging chalcogen is only an indirect one.[15,49] There are also cases where the effect of S/Se substitution on oxidation potentials is negligible as in the case of $[Mo_4Se_4(edta)_2]^{n-}$ as compared to $[Mo_4S_4(edta)_2]^{n-}$ ($n = 4, 3, 2$) where the difference is no more than 5 mV. The substitution more often than not results in positive shifts (upto 60 mV) as has been demonstrated for the $Fe_2Se_2$ and $Fe_4Se_4$ cores, where the direction of the potential shift can also depend on the terminal ligands.[52,53] For the series $[(MeC_5H_4)_4Ru_4E_4]^{n+}$ (E = S, Se, Te; $n = 0, 1, 2$) substitution of the heavier chalcogen shifts the potential to more negative values for the 1+/2+ couple, but for the 0/1+ couple the shift is positive with the effect that the two waves coalesce for E = Te.[46]

The 4+/5+ couples have $\Delta E$ values close enough to the standard 59 mV with $I_a/I_c$ ratios close enough to unity to be described as reversible. The 5+/6+ couples on the contrary have $I_a/I_c$ ratios between 1 and 2, depending on the scan speed, with cathodic and anodic peak separation of 60−90 mV, and are quasi-reversible. A possible explanation of the difference may be that removing one electron from a 5+ species (11 cluster

(52) Patrick, M. A.; Laskowski, E. J.; Johnson, R. W.; Gillum, W. O.; Berg, J. M.; Hodgson, K. O.; Holm, R. H. *Inorg. Chem*. **1978**, *17*, 1402.

(53) Yu, S.-B.; Papaethymiou, G. C.; Holm, R. H. *Inorg. Chem*. **1991**, *30*, 3476.

electrons) is accompanied by a greater distortion of the $M_4$ tetrahedral skeleton than it does when an electron is removed from a 4+ species. Thus, in the highly distorted 6+ core in $[W_4Te_4(CN)_{12}]^{6-}$ the longest and shortest W−W distances differ by 0.215 Å whereas for the much less distorted 5+ core in $[Mo_4Te_4(CN)_{12}]^{7-}$ this difference is only 0.03 Å (see Table 7). For the electron-precise $W_4E_4^{4+}$ clusters one would expect little or no distortion.

That the $Mo_4Te_4$ cube shows much higher potentials for both oxidation waves is consistent with greater stability of higher oxidation states for 5d transition elements compared with those for the 4d series. For aqua cubes, heterometallic $[W_3MoE_4(H_2O)_{12}]^{n+}$ (E = S, Se) display negative shifts of about 500−600 mV for both 4+/5+ and 5+/6+ waves, compared to their $Mo_4E_4$ analogues.[38] Again, in the case of octahedral $[M_6S_8(PEt_3)_6]^{n+}$ ($n = -1, 0, 1$; M = Mo, W), the W cluster shows a negative shift of 200−300 mV.[54] Although information about electrochemical behavior in other 4d/5d pairs of structural analogues is not very common, in the case of the trinuclear acetato-bridged $[M_3(\mu_3\text{-}O)(\mu\text{-}OAc)_6(py)_3]^+$ complexes (M = Rh, Ir; py = pyridine) the Rh complex undergoes reversible one-electron oxidation at a 640 mV higher potential than its Ir analogue.[55]

**Acknowledgment.** This work was supported by the Russian Foundation for Basic Research (research grant No. 96-03-33018 for the Novosibirsk team), European Union INTAS (research grant No. 96-1256), and the UK Engineering and Physical Sciences Research Council.

**Supporting Information Available:** X-ray crystallographic files, in CIF format, for the structure determination of **1**-**5**. This material is available free of charge via the Internet at http://pubs.acs.org.

IC980956Z

(54) Saito, T.; Yoshikava, A.; Yamagata, T.; Imoto, H.; Unoura, K. *Inorg. Chem*. **1989**, *28*, 3588.
(55) Tahahashi, K.; Umakoshi, K.; Kikuchi, A. Sasaki, Y.; Tominaga, M.; Taniguchi, I. *Z. Naturforsch.* **1995**, *50b*, 551.